RNA Conformation in Catalytically Active Human Telomerase

Justin A. Yeoman,[†,¶] Angel Orte,[†,§] Beth Ashbridge,[†] David Klenerman,[*,†] and Shankar Balasubramanian[*,†,‡]

[†]*The University Chemical Laboratory, University of Cambridge, Lensfield Road, Cambridge CB2 1EW, U.K., and* [‡]*School of Clinical Medicine, University of Cambridge, Cambridge CB2 0SP, U.K.*

Current addresses: [¶]*National Centre for Biological Sciences, Tata Institute of Fundamental Research, UAS GKVK, Bellary Road, Bangalore 560 065, India, and* [§]*Department of Physical Chemistry, Faculty of Pharmacy, Campus Cartuja, Granada 18071, Spain.*

*E-mail: sb10031@cam.ac.uk, dk10012@cam.ac.uk

SUPPORTING INFORMATION

for a Communication to the

Journal of the American Chemical Society

Contents

1. General experimental section

All chemicals and biological reagents were molecular biology grade and purchased from Sigma-Aldrich, and all enzymes were purchased from New England BioLabs, unless stated otherwise. Water was molecular biology grade (DNase-, RNase-free) and purchased from Sigma-Aldrich. Milli-Q water was filtered through a Milli-Q® Gradient System (Millipore, Watford, U.K.) to 18.2 mΩ purity. The composition of a number of buffer solutions employed in this work is detailed in Table S1.

Dual-labeled RNA preparation

Experimental details for preparation of the full-length dual-labeled hTR construct are presented in Supporting Information Section 2.

Preparative denaturing polyacrylamide gel purification

The ssRNA sample to be purified was run on a medium-sized denaturing polyacrylamide gel. The RNA pellet of the sample to be purified was reconstituted in 30 μL non-dye urea loading buffer. Immediately prior to loading, the sample was heated at 90°C for 3 min then kept on ice for 2 min. The gel was run in a vertical fashion then visualized between two sheets of laboratory plastic wrap on a preparative tlc plate under 365 nm illumination in a UV light box. The position of the RNA band of interest was marked with a marker pen and the piece of gel containing the RNA was excised using a scalpel. The time the RNA was exposed to UV illumination was kept to a minimum.

Table S1. Buffer solution composition.

Buffer solution	Composition
Non-dye urea loading buffer	5 mM Tris.HCl, pH 7.4, 20 mM EDTA, 8 M urea
Gel elution buffer	20 mM Tris.HCl, pH 8.0, 300 mM NaCl, 2 mM EDTA, 0.25% (w/v) SDS
Labeling Buffer	50 mM Tris.HCl, pH 7.6, 50 mM NaCl, 1 mM EDTA
Wash Buffer A	50 mM Tris.HCl, pH 7.4, 100 mM KCl, 5 mM $MgCl_2$, 1 mM EDTA, 10% (v/v) glycerol
Wash Buffer B	50 mM Tris.HCl, pH 7.4, 100 mM KCl, 1 mM $MgCl_2$, 10% (v/v) glycerol, 0.1 mg/mL BSA, 0.01 mg/mL yeast tRNA
Blocking Buffer A	50 mM Tris.HCl, pH 7.4, 100 mM KCl, 5 mM $MgCl_2$, 10% (v/v) glycerol, 0.5 mg/mL BSA, 0.1 mg/mL yeast tRNA
Blocking Buffer B	100 mM Tris.HCl, pH 7.4, 200 mM KCl, 10 mM $MgCl_2$, 20% (v/v) glycerol, 1 mg/mL BSA, 0.2 mg/mL yeast tRNA
Elution Buffer A	50 mM Tris.HCl, pH 7.4, 100 mM KCl, 5 mM $MgCl_2$, 1 mM EDTA, 10% (v/v) glycerol, 0.3 mg/mL 3× FLAG peptide, 0.1 mg/mL BSA
Dilution Buffer	25 mM Tris.HCl, pH 7.4, 50 mM KCl, 5 mM $MgCl_2$, 1 mM EDTA, 0.02 mg/mL BSA, 0.01 mg/mL yeast tRNA

The excised gel fragment was transferred to a 1.7 mL microcentrifuge tube and crushed with an autoclaved micropestle. An initial 1 mL gel elution buffer was added and the resulting suspension incubated at –80°C until frozen, thawed at 50°C and heated at 90°C for 5 min. The RNA was eluted from the gel at room temperature with shaking for ~16 h. The suspension was centrifuged at 12,066 × g for 5 min to collect the gel particles at the bottom of the tube and the supernatant was removed and kept on ice. A further 0.5 mL gel elution buffer was added to the tube and a second elution performed at room temperature with shaking for ~6 h. The suspension was centrifuged at 12,066 × g for 5 min and the supernatant removed. The combined supernatants were passed through a 0.22 μm syringe filter to remove any remaining gel particles and the volume was reduced via butanol extraction from ~1.5 mL to 400 μL. Ethanol precipitation was performed and the RNA pellet was reconstituted in water.

Coupled in vitro transcription/translation of hTERT

Protein was expressed and an RNP complex reconstituted in a cell-free TNT® T7 Quick Coupled Transcription/Translation System (Promega, Southampton, U.K.). To 100 μL TNT® Quick Master Mix was added 2.5 μg of the expression vector pET28-3×FLAG-hTERT, 10 pmol dual-labeled RNA and 2 nmol methionine. The expression mixture had a total reaction volume of 125 μL and was incubated at 30°C for 2 h.

Affinity-based hTERT purification

The RNP complex formed during coupled in vitro transcription/translation was purified via an integral N-terminal 3× FLAG tag. All steps of the purification were performed at

4°C. A 1.7 mL microcentrifuge tube was loaded with 50 µL anti-FLAG® M2 affinity gel suspension and centrifuged at 706 × g for 1 min. The supernatant was removed and 500 µL Wash Buffer A added. The tube was inverted by hand 10 times, centrifuged at 706 × g for 1 min, and the supernatant was removed. The gel was washed a further four times according to the same protocol. 500 µL Blocking Buffer A was added and the microcentrifuge tube inverted at 12 rpm on a rotator for 30 min. The tube was centrifuged at 706 × g for 1 min and the supernatant was removed. The gel was blocked a second time for 30 min according to the same protocol. In parallel, after the protein expression and RNP complex reconstitution, 125 µL Blocking Buffer B was added to the expression mixture, the microcentrifuge tube inverted 5 times, and the blocking mixture centrifuged at 16,708 × g for 20 min. The supernatant was removed from any precipitated material and applied to the blocked anti-FLAG® affinity gel. The tube containing the gel was inverted at 12 rpm on a rotator overnight. The following day, the gel was washed 6 times with 500 µL Wash Buffer B according to the same protocol used during gel preparation. 150 µL Elution Buffer A was added to the gel and the tube inverted at 12 rpm on a rotator for 60 min. The tube was centrifuged at 706 × g for 1 min and the supernatant was removed and divided into 5 × 30 µL aliquots. The aliquots of dual-labeled RNA/hTERT preparation were snap-frozen and stored at –80°C.

Single-molecule optical experiments

Each dual-labeled hTR construct and dual-labeled RNA/hTERT preparation was analyzed in solution by fluorescence microscopy at the single-molecule level. Single-molecule TCCD-1ex measurements were performed on a home-built two-color confocal

inverted microscope set-up.[1] The set-up incorporated a single multi-line argon/krypton laser (model 35 LDL 840-240, Melles Griot, Cambridge, U.K.). In a TCCD-1ex measurement a single laser line, 488 nm, was directed to the back port of an inverted microscope (model Eclipse TE2000-U, Nikon, Kingston upon Thames, Surrey, U.K.). The laser beam was focused 6 μm into the sample solution through an oil immersion objective lens (NA 1.45, model Plan Apochromat TIRF 60×, Nikon). Fluorescent light emitted by the sample was collected back through the objective lens and directed to a 50 μm pinhole (Melles Griot). The pinhole rejected out of focus fluorescent and other background light and defined the probe volume within the sample solution from which a fluorescence signal was recorded. The remaining light was separated according to wavelength by a dichroic mirror (model 585DRLP, Omega Optical, Brattleboro, Vermont, U.S.), filtered in each channel by appropriate longpass and bandpass filters, and focused onto two avalanche photodiodes (SPCM AQR-14, Perkin-Elmer Optoelectronics, Cambridge, U.K.). The signal from each avalanche photodiode was processed using a separate MCS card and the two signals were cross-correlated. The sample to be analyzed was diluted on the microscope stage to between 10 and 50 pM in Dilution Buffer in a total volume of either 1 mL in a chambered coverglass or 200 μL on a simple coverglass. Data were collected with a 1 ms time bin on both MCS cards then subjected to background correction, thresholding and analysis for coincidence as described previously.[1–4]

Apparent FRET efficiency information relating to a coincident species was extracted through analysis of the coincidence histogram. The function $Z = \ln(I_A/I_D)$ was plotted

where I_A and I_D are the background and cross-talk corrected intensities of coincident events in the acceptor and donor channels respectively. The resulting frequency distribution was fit with one or more normal distribution functions. The central position of a particular fitted normal distribution peak, x_c, can be converted to an equivalent proximity ratio, P, by substituting x_c into the equation for the proximity ratio, Equation S1, to give Equation S2.

$$P = I_A/(I_D + I_A) \quad \text{(S1)}$$

$$P = e^{xc}/(1 + e^{xc}) \quad \text{(S2)}$$

The inclusion of an extra normal distribution function in the fitting process was justified by a decrease in the goodness-of-fit parameter χ^2 of > 20% upon addition of an extra peak and by *F* tests to compare two- versus three-peak models.

F tests were performed as follows. The *F* ratio accounts for the relative decrease in the sum of squares with respect to the decrease in degrees of freedom when a more complicated model is used to fit the same set of data. The *F* ratio is given by Equation S3.

$$F = \frac{\left(SS_{null} - SS_{alt}\right)/\left(dof_{null} - dof_{alt}\right)}{S_{alt}/dof_{alt}} \quad \text{(S3)}$$

SS and *dof* are the sum of squares and the degrees of freedom respectively of either the null hypothesis (two Gaussian peaks function) or the alternative model (three Gaussian peaks function). A critical *F* value is calculated for a 0.05 significance level, and the critical *F* value is compared to the calculated value for the fits of the data. If the *F* ratio

obtained surpasses the critical *F* this indicates there is less than a 5% probability that the improvement of the fitting using the alternative model is due to chance. Therefore, if the calculated *F* ratio is higher than the critical *F* value, the alternative model (i.e. the three-peak function) can be considered statistically more correct. Figure S1 shows a number of examples of *F* ratios obtained from fitting TCCD histograms generated from dual-labeled hTR data, in the presence and absence of hTERT, with two or three Gaussian functions. In the absence of hTERT the *F* values were always below the critical *F*, meaning no statistical improvement was achieved from use of three Gaussian functions in the fitting. However, Figure S1 clearly shows the high *F* ratio values obtained when hTERT was present. The *F* ratios obtained in these cases always indicated that the probability that the three-peaks model was correct was higher than 99.9% (considerably higher than the critical criteria set at 95% for a significance level of 0.05).

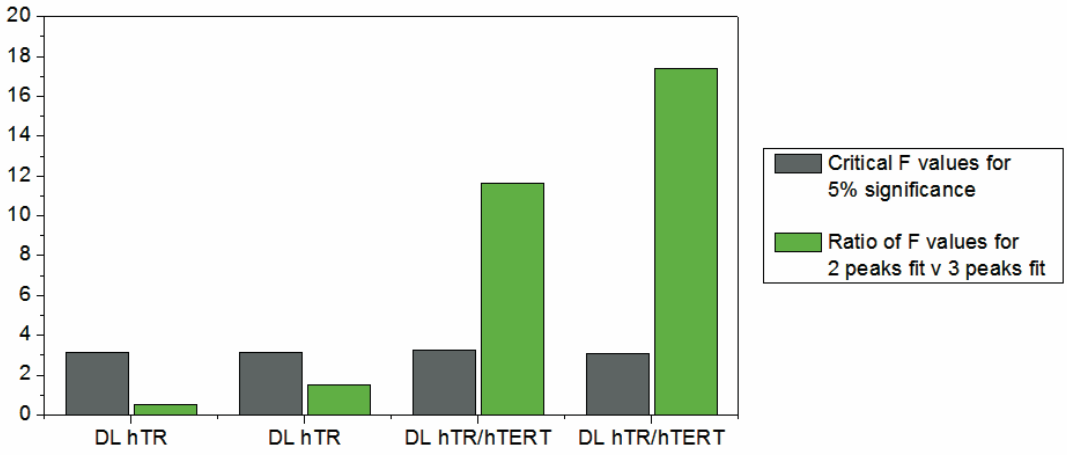

Figure S1. *F* tests for two-peak (null hypothesis) versus three-peak (alternative hypothesis) fitting function fits of TCCD histograms for **DL hTR** in the absence or presence of hTERT. Ratios of critical *F* values (green bars) for a 0.05 significance compared to ratios of calculated *F* values (grey bars). The three-peak fitting function is only significant for **DL hTR** in the presence of hTERT.

Steady-state fluorescence measurements

Steady-state fluorescence emission spectra were collected at 20°C on a Jasco FP-6500 fluorescence spectrophotometer equipped with a 450 W xenon lamp and Peltier temperature controller ETC-273T.

Time-resolved fluorescence measurements

Fluorescence decay traces of **DL hTR** in solution were recorded in Time-Correlated Single Photon Counting (TCSPC) mode using a FluoTime 200 fluorescence lifetime spectrometer (PicoQuant GmbH, Berlin, Germany). The excitation source was a pulsed 470 nm laser (LDH-P-C-470, PicoQuant GmbH) with a 20 MHz repetition rate controlled by a PDL-828 'Sepia II' driver unit (PicoQuant GmbH). Fluorescence was collected beyond a polarizer set at the magic angle and a 2 nm bandwidth monochromator to select the emission wavelength. A TimeHarp 200 PC-board (PicoQuant GmbH) was used to collect the discriminated signal and plot fluorescence decay histograms over 1320 channels with a time increment per channel of 36 ps. The collected emission wavelengths were 515, 525, 535, 545, and 555 nm for the donor (Alexa Fluor® 488) decay traces, and 615, 625, and 635 nm for the acceptor (Alexa Fluor® 594) decay traces. The histograms were typically recorded until they reached a maximum of 2×10^4 counts. The decay traces were analyzed by a least squares based deconvolution method in terms of multi-exponential functions using FluoFit software (PicoQuant GmbH), employing instrument response functions collected using Ludox scatterer. The five traces from the donor fluorophore were fit globally with the decay times linked as shared parameters, whereas the pre-exponential factors were local adjustable parameters. The analyses were

performed in the same manner for the three traces from the acceptor fluorophore in each sample. The quality of each fit was judged by measuring the reduced χ^2 value and the randomness in the distributions of weighted residuals and autocorrelation functions.

2. Synthesis of DL hTR

The synthetic strategy for preparation of **DL hTR** is summarized in Figures S2–3. The sequences of the PCR primers and hTR fragments employed in the synthesis of **DL hTR** are detailed in Table S2.

hTR fragment preparation

i) 5' fragment preparation

Deletion of the single-stranded section at the hTR 5' end does not lead to a reduction in telomerase activity in vitro.[5] It was therefore decided to delete the first 14 nt of this section and attach the donor fluorophore, Alexa Fluor® 488, to a truncated hTR 5' end. It was hypothesized that minimizing the distance between the donor fluorophore and the stable structural motif of helix P1 would reduce the conformational freedom of the fluorophore and thereby improve the accuracy with which the separation of donor and acceptor fluorophores could be recorded.

The sequence coding for hTR nt 15-109 was amplified by PCR using the forward primer hTR15-109F, the reverse primer hTR15-109R and the plasmid pUC18-hTR as a template. The PCR product was double restriction endonuclease digested with HindIII and BamHI and sub-cloned into the pUC18 vector to create the new construct pUC18-hTR(15-109). The plasmid pUC18-hTR(15-109) was linearized with BamHI.

The hTR 5' fragment modified with a sulfur atom at the γ-phosphate of the 5' end nucleotide, hTR(15-109)-γ-S, was synthesized by run-off in vitro transcription using T7

RNA polymerase. 8 µg linearized pUC18-hTR(15-109) plasmid DNA was used as a template by 400 U T7 RNA polymerase (Agilent Technologies, Stockport, U.K.) in a 200 µL reaction containing 193 U ribonuclease inhibitor and 40 mM Tris.HCl, pH 8.0, 50 mM NaCl, 12 mM $MgCl_2$, 2 mM spermidine, 40 mM DTT, 3 mM ATP, 3 mM CTP, 3 mM TTP, 3 mM GTP-γ-S. The reaction mixture was incubated at 37°C for 2 h. 20 U DNase I were added and the reaction mixture incubated at 37°C for 20 min. The solution was subjected to phenol:chloroform extraction and the RNA purified via an RNeasy Protect Mini Kit (QIAGEN, Crawley, U.K.) following the manufacturer's protocol with the modification that two extra washes with 500 µL Buffer RPE were carried out. Finally, an ethanol precipitation was performed and the air-dried RNA pellet reconstituted in an appropriate volume of freshly degassed Labeling Buffer.

hTR(15-109)-γ-S was site-specifically labeled at the 5' end by reaction with the maleimide derivative of Alexa Fluor® 488 (Invitrogen, Paisley, U.K.). 1 mg Alexa Fluor® 488 C_5 maleimide, 1.39 µmol, dissolved in 25 µL DMSO, was combined with 174 µg hTR(15-109)-γ-S, 5.55 nmol, dissolved in 75 µL Labeling Buffer, in a 250 : 1 molar ratio and a 100 µL total reaction volume. The reaction mixture was incubated at 30°C for 2 h 30 min in the dark. After reaction, unincorporated fluorescent dye molecules were removed via an RNeasy Protect Mini Kit (QIAGEN) following the manufacturer's protocol with the modification that two extra washes with 500 µL Buffer RPE were carried out.

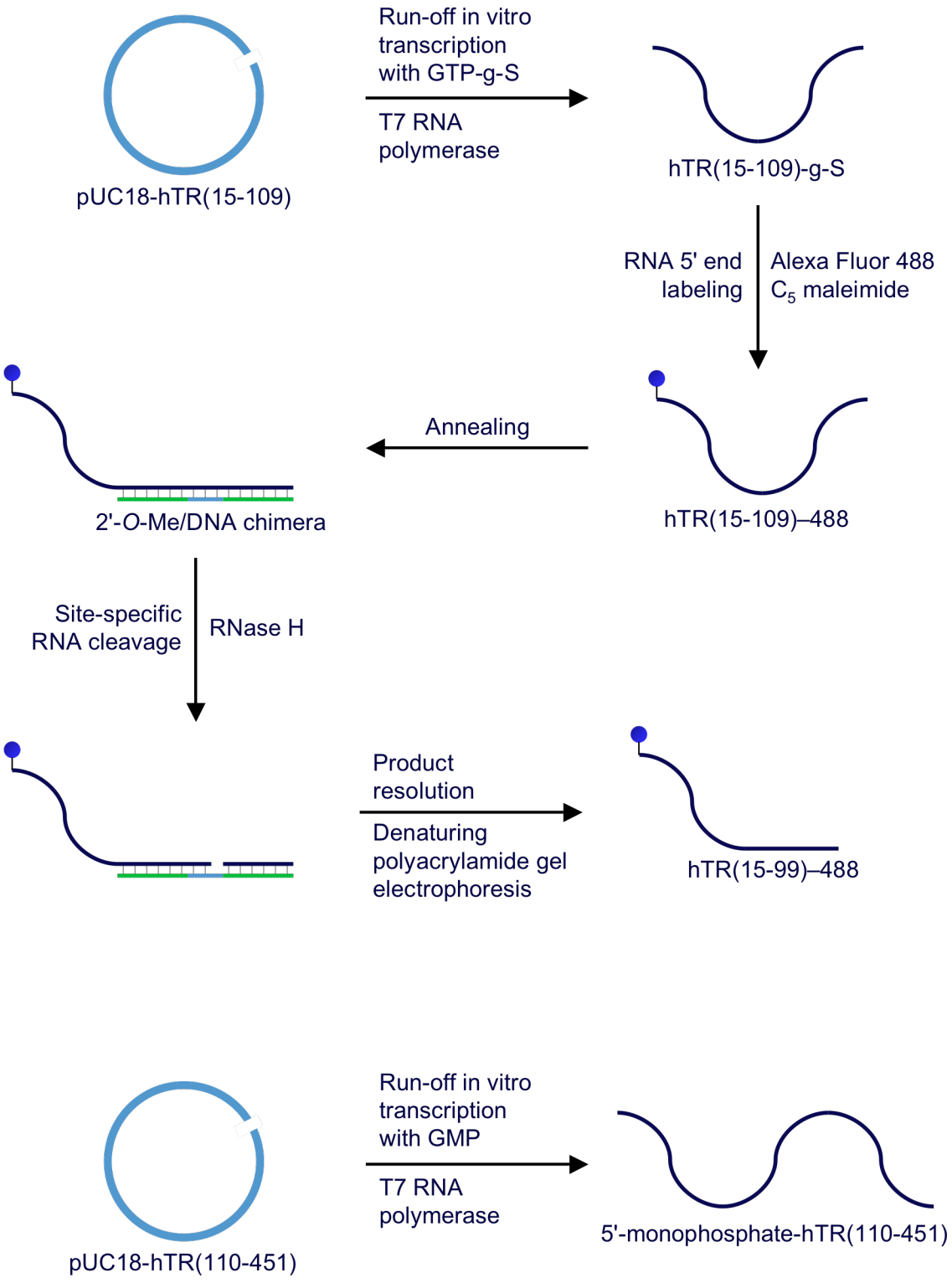

Figure S2. Synthetic scheme for preparation of hTR 5' and 3' fragments.

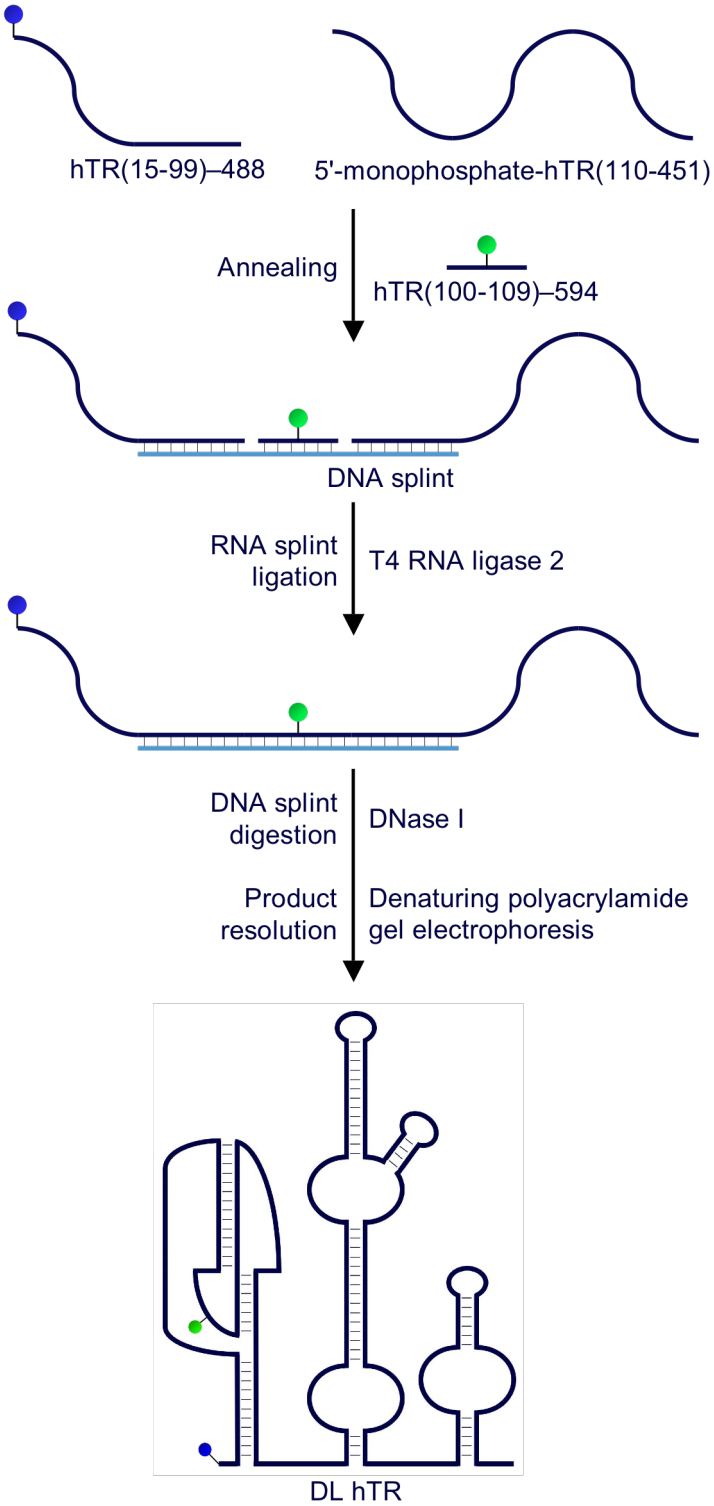

Figure S3. Synthetic scheme for ligation and purification of **DL hTR**.

3' end heterogeneity of hTR(15-109)–488 labeled in vitro transcripts was eliminated via site-specific RNA cleavage using a cut-directing chimeric oligonucleotide and the enzyme RNase H. 600 pmol hTR(15-109)–488 was combined with 1.2 nmol 2'-*O*-Me/DNA chimeric oligonucleotide in a 1 : 2 molar ratio and a total volume of 180 µL. The oligonucleotide was designed to be complementary to the RNA 3' end and to contain a central 4 nt DNA flanked by 2'-*O*-Me RNA. The RNA and chimeric oligonucleotide were annealed together: they were heated at 90°C for 5 min then incubated at 37°C for 15 min. 60 U RNase H were added and the solution made up to a total reaction volume of 400 µL containing 240 U ribonuclease inhibitor and 1× RNase H Reaction Buffer, 50 mM Tris.HCl, pH 8.3, 75 mM KCl, 3 mM $MgCl_2$, 10 mM DTT. The reaction mixture was incubated at 37°C for 1 h, followed by phenol:chloroform extraction and ethanol precipitation. The nucleic acid pellet was reconstituted in 15 µL non-dye urea loading buffer and the product hTR(15-99)–488 subjected to preparative denaturing polyacrylamide gel purification.

ii) 3' fragment preparation

The sequence coding for hTR nt 110-451 was amplified by PCR using the forward primer hTR110-451F, the reverse primer hTR110-451R and the plasmid pUC18-hTR as a template. The PCR product was double restriction endonuclease digested with HindIII and BamHI and sub-cloned into the pUC18 vector to create the new construct pUC18-hTR(110-451). The plasmid pUC18-hTR(110-451) was linearized with BamHI. hTR(110-451) 5' monophosphate, 5'-monophosphate-hTR(110-451), was synthesized by runoff in vitro transcription using T7 RNA polymerase and linear pUC18-hTR(110-451)

as a template. 8 μg linear pUC18-hTR(110-451) was used as a template by 400 U T7 RNA polymerase in a 200 μL reaction containing 193 U ribonuclease inhibitor and 40 mM Tris.HCl, pH 8.0, 50 mM NaCl, 12 mM $MgCl_2$, 2 mM spermidine, 40 mM DTT, 1 mM ATP, 1 mM CTP, 1 mM TTP, 1 mM GTP, 20 mM GMP. The reaction and purification conditions used for 5'-monophosphate-hTR(110-451) were the same as for synthesis of hTR(15-109)-γ-S.

iii) Middle fragment preparation

A PAGE purified synthetic RNA oligonucleotide, hTR(100-109)–594, with the same sequence as hTR nt 100-109, internally modified on nt 105 with a deoxyribose sugar and an Alexa Fluor® 594 fluorophore (Invitrogen) attached to the uracil base, was purchased (IBA GmbH, Göttingen, Germany).

RNA ligation

Three pieces of RNA were ligated together simultaneously using a single DNA splint and the enzyme T4 RNA Ligase 2. 200 pmol each of the shortest two pieces of RNA, hTR(15-99)–488 and hTR(100-109)–594, were combined with 105 pmol of the longest piece of RNA, 5'-monophosphate-hTR(110-451), and 200 pmol of the 100 nt DNA splint in a 2 : 2 : 1 : 2 molar ratio and a total volume of 100 μL, containing NaCl at a concentration of 100 mM. The four nucleic acid molecules were annealed together: they were heated at 95°C for 5 min then incubated at 30°C for 10 min. 50 U T4 RNA Ligase 2 were added and the solution made up to a total reaction volume of 200 μL containing 240 U ribonuclease inhibitor and 1× T4 RNA Ligase 2 Reaction Buffer, 50 mM Tris.HCl,

pH 7.5, 2 mM $MgCl_2$, 1 mM DTT, 400 μM ATP. 2 × 200 μL reaction mixtures were prepared in parallel and incubated at 30°C for 90 min. 20 U DNase I were added to each and they were incubated at 37°C for 20 min, before being combined into one volume. Phenol:chloroform extraction and ethanol precipitation were performed, the nucleic acid pellet was reconstituted in 30 μL non-dye urea loading buffer and the products were subjected to preparative denaturing polyacrylamide gel purification. Analytical gel images of purified **DL hTR** are presented in Figure S4.

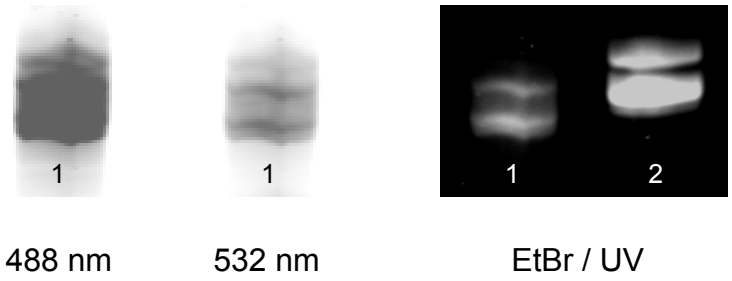

Figure S4. Analytical gel images of purified dual-labeled full-length hTR construct **DL hTR**. Lane 1, dual-labeled hTR construct; lane 2, unlabeled wt hTR. The visibility of bands under excitation at 488 and 532 nm demonstrates that both donor and acceptor fluorophores are present. The dual-labeled hTR construct (437 nt) has a marginally higher mobility than the unlabeled wt hTR (451 nt). The appearance of full-length hTR as a doublet in polyacrylamide gels, even under denaturing conditions, has been reported in the literature.[6]

Table S2. PCR primer and hTR fragment sequences.

DNA primer or RNA fragment	Sequence
Primer hTR15-109F	5'-TAC TGT AAG CTT TAA TAC GAC TCA CTA TAG GGC CTG GGA GGG GTG GTG GC-3'
Primer hTR15-109R	5'-TAC TGT GGA TCC AGC GAG AAA AAC AGC GCG CGG-3'
Primer hTR110-451F	5'-TAC TGT AAG CTT TAA TAC GAC TCA CTA TAG ACT TTC AGC GGG CGG AAA AGC-3'
Primer hTR110-451R	5'-TAC TGT GGA TCC GCA TGT GTG AGC CGA GTC CTG G-3'
Fragment hTR(15-109)	5'-GGG CCU GGG AGG GGU GGU GGC CAU UUU UUG UCU AAC CCU AAC UGA GAA GGG CGU AGG CGC CGU GCU UUU GCU CCC CGC GCG CUG UUU UUC UCG CU-3'
Fragment hTR(110-451)	5'-GAC UUU CAG CGG GCG GAA AAG CCU CGG CCU GCC GCC UUC CAC CGU UCA UUC UAG AGC AAA CAA AAA AUG UCA GCU GCU GGC CCG UUC GCC CCU CCC GGG GAC CUG CGG CGG GUC GCC UGC CCA GCC CCC GAA CCC CGC CUG GAG GCC GCG GUC GGC CCG GGG CUU CUC CGG AGG CAC CCA CUG CCA CCG CGA AGA GUU GGG CUC UGU CAG CCG CGG GUC UCU CGG GGG CGA GGG CGA GGU UCA GGC CUU UCA GGC CGC AGG AAG AGG AAC GGA GCG AGU CCC CGC GCG CGG CGC GAU UCC CUG AGC UGU GGG ACG UGC ACC CAG GAC UCG GCU CAC ACA UGC-3'

Fragment hTR(100-109)–594	5'-UUU UCdU(Alexa Fluor® 594) CGC U-3'
2′-*O*-Me/DNA chimera	5'-mAmGmC mGmAmG mAmAmA mAdAdC dAdGmC mGmCmG mCmG-3'
DL hTR 100-*mer* DNA splint	5'-ACG GTG GAA GGC GGC AGG CCG AGG CTT TTC CGC CCG CTG AAA GTC AGC GAG AAA AAC AGC GCG CGG GGA GCA AAA GAC GGC GCC TAC GCC CTT CTC AGT-3'

3. TRAP assay

The presence of telomerase activity within a sample was assayed via Telomerase Repeat Amplification Protocol (TRAP) using the TRAPeze® Telomerase Detection Kit (Millipore). A primer extension reaction was performed using the sample in a 25 μL total volume containing TS Primer, 50 μM each dNTP and 1× TRAP Reaction Buffer, 20 mM Tris.HCl, pH 8.3, 63 mM KCl, 1.5 mM $MgCl_2$, 1 mM EGTA, 0.05% Tween-20. After reaction, the DNA products were purified via a QIAquick® Nucleotide Removal Kit (QIAGEN) following the manufacturer's protocol. The product solution was lyophilized and the products reconstituted in 30 μL water. A PCR was performed using 1.6 U *Taq* DNA Polymerase and the product solution in a 40 μL total volume containing radiolabeled TS Primer, modified with a ^{32}P atom at the α-phosphate of the 5' end nucleotide, RP primer, K1 primer, TSK1 template, 50 μM each dNTP and 1× TRAP Reaction Buffer, 20 mM Tris.HCl, pH 8.3, 63 mM KCl, 1.5 mM $MgCl_2$, 1 mM EGTA, 0.05% Tween-20. The reaction was performed in a Techne TC-512 thermal cycler using a standard PCR program: 94°C for 5 min, 30× three-step cycles of 94°C for 30 s, 59°C for 30 s, 72°C for 30 s, then hold at 4°C. After reaction, the PCR products were resolved by analytical non-denaturing polyacrylamide electrophoresis. Telomerase activity was quantitated by densitometric analysis using ImageQuant™ TL analysis software (GE Healthcare). The total signal of the telomerase ladder was background corrected and expressed relative to the background corrected TSK1 signal from the same lane.

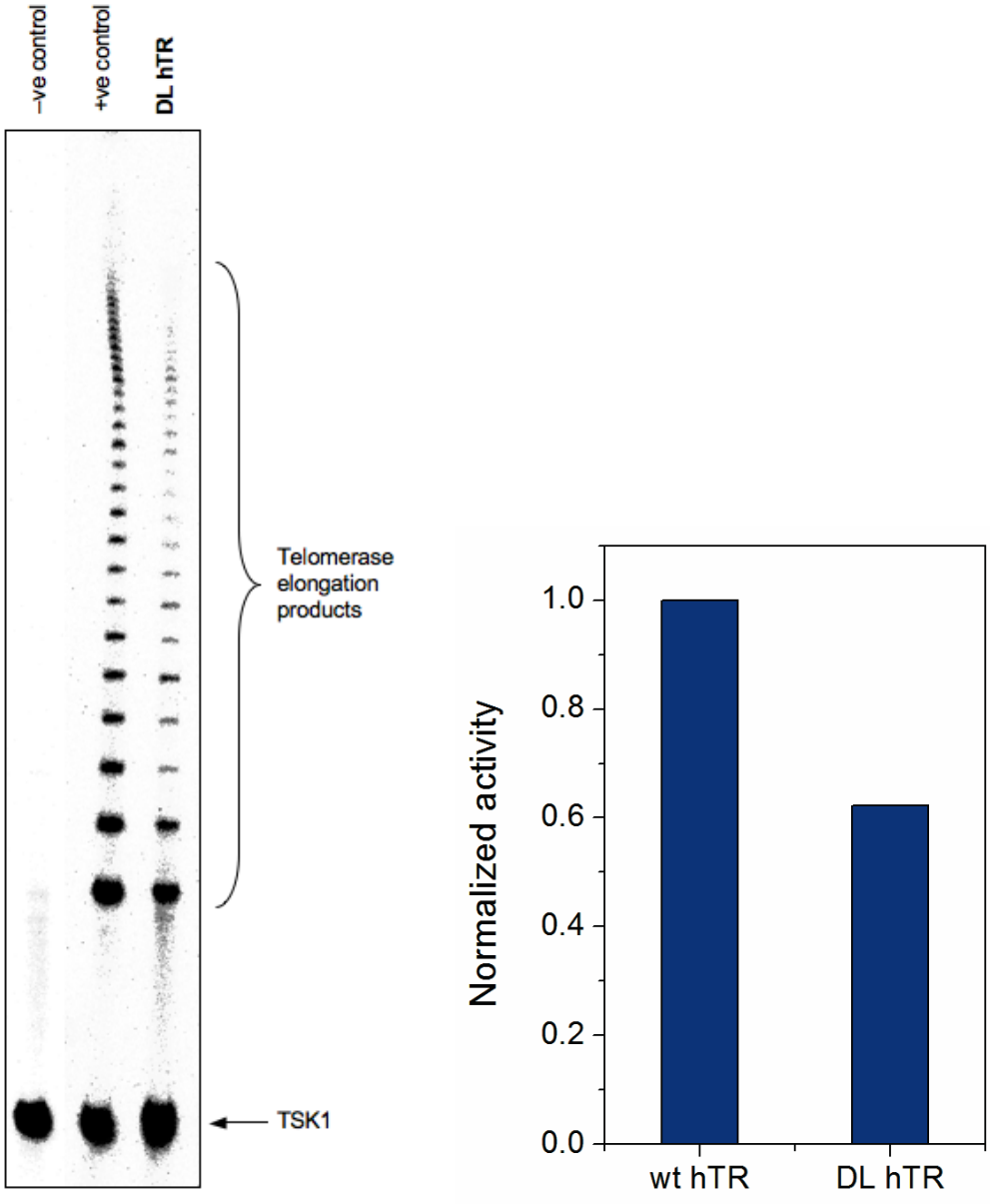

Figure S5. Left, activity of the **DL hTR**•hTERT telomerase complex subjected to single molecule TCCD-1ex analysis in this work, as assayed by TRAP. The negative control was CHAPS lysis buffer and the positive control was a telomerase complex containing wt hTR. Right, quantitation of telomerase activity supported by the dual-labeled hTR construct. A telomerase complex containing **DL hTR** retains > 50% the activity of one containing wt hTR.

4. Estimate of DL hTR interfluorophore distance

Two structures deposited in the RCSB Protein Data Bank were employed in our analysis: 2K95 'Solution structure of the wild-type P2B-P3 pseudoknot of human telomerase RNA'[7] and 2INA 'Theoretical model for Human Telomerase RNA Monomer from FRET measurements'.[8] Wherever possible, information was used from 2K95; these data were derived by solving the solution structure of the wt minimal hTR pseudoknot construct by NMR and demonstrate a network of tertiary contacts between pseudoknot loops and helices that act to compress the structure into something resembling a triple helix. Otherwise, information was used from 2INA; these data were derived by constructing a molecular model of the entire 5' half of hTR based on a set of distance parameters derived from fluorescently labeled PNA hybridization probes.

Our analysis was performed according to the following procedure. Nucleotide numbering is as per full-length wt hTR. Distances were measured between the phosphorus atom of the phosphate group 5' to the nucleotide in question. The length of the linker between the labeled nucleotide and the fluorophore was not taken into account.

1) Take the distance from nucleotide G(15) to nucleotide C(183) in 2INA = 38.90 Å. In **DL hTR** the donor fluorophore is attached to G(15), 3 nt away from the end of helix P1 distal to the pseudoknot. C(183) is the nucleotide at the 3' end of helix P3 and the pseudoknot as a whole.

2) Take the distance from nucleotide C(183) to nucleotide U(105) in 2K95 = 13.92 Å. In **DL hTR** the acceptor fluorophore is attached to U(105) in loop J2b/3.

3) Assume that G(15), C(183) and U(105) are collinear and estimate the distance between G(15) and U(105) in full-length hTR as 38.90 Å + 13.92 Å = 52.82 Å.

4) Use the R value from 3) in conjunction with the R_0 value for the donor and acceptor of 60 Å(Ref. 9) to calculate the proximity ratio and thereby estimate the FRET efficiency using proximity ratio = $1/(1 + (R/R_0)^6) = 0.68$.

5) Trigonometric analysis allows a prediction of the effect of varying the angle between the G(15)–C(183) and C(183)–U(105) vectors on FRET efficiency. Variation of the G(15)–C(183)–U(105) angle from 180° to 150° results in a decrease of the distance between G(15) and U(105) from 52.82 Å to 51.26 Å and a corresponding increase of the FRET efficiency estimate to 0.72.

The value obtained in 4) is in good agreement with our experimentally determined proximity ratio for **DL hTR** complexed with hTERT of 0.67.

5. Additional FRET data

Single-molecule measurements

Single-molecule data for **DL hTR**, in either the absence or presence of hTERT, were processed to produce a conventional proximity ratio histogram, Figure S6, in order to allow a comparison with the TCCD-1ex data processing. The use of an OR criterion, as opposed to the AND criterion used to generate TCCD-1ex plots, leads to the presence of more histogram intensity at extreme FRET efficiencies, in particular at low FRET where the ubiquitous 'zero peak' can be seen. For the dual-labeled hTR data presented in this article, the AND criterion is a more stringent filtration method and leads to simpler histograms. In addition, a histogram generated by subtraction of the normalized **DL hTR** only TCCD histogram from the normalized **DL hTR**•hTERT TCCD histogram is presented in Figure S7. This differential histogram shows the disappearance of the population(s) at low FRET efficiency, i.e. at negative values of $\ln(I_A/I_D)$, and the concomitant increase of the contribution at higher FRET efficiency.

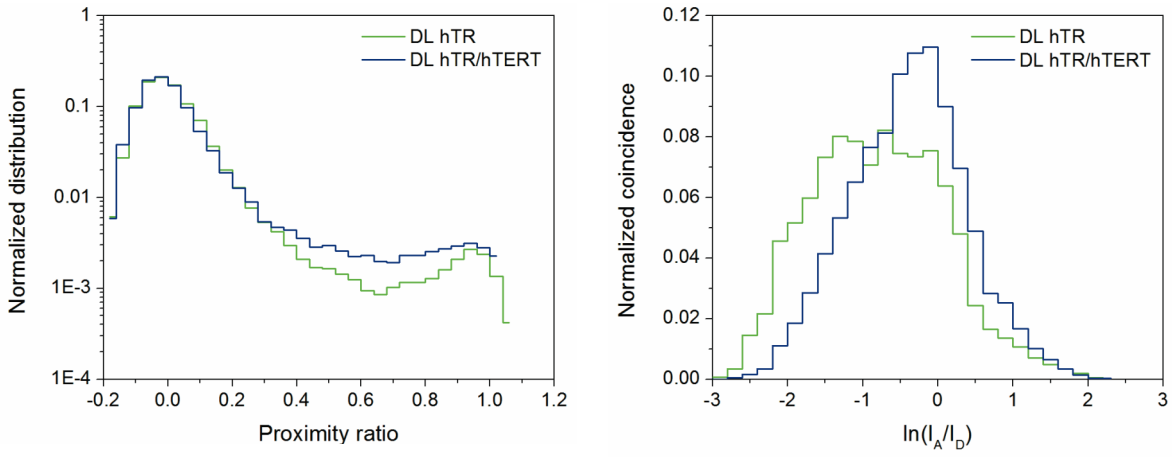

Figure S6. Comparison of conventional proximity ratio (left) and Two-Color Coincidence Detection (right) histograms for **DL hTR**, either alone (green) or complexed with hTERT (blue).

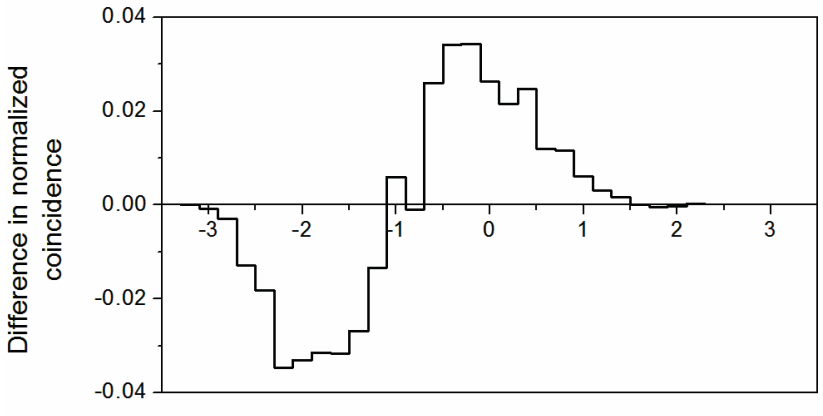

Figure S7. Difference between normalized TCCD-1ex histograms in the presence and absence of hTERT.

Fluorescence emission spectra

Bulk emission spectra for **DL hTR** showed a low level of FRET on average: very little emission from the acceptor fluorophore was obtained upon excitation of the donor, Figure S8. This confirmed the fact that the majority of the dual-labeled hTR population displayed a much lower FRET efficiency than that expected as a result of helix P3 base-pairing and hTR pseudoknot formation (see Figures 1a and b of the main manuscript).

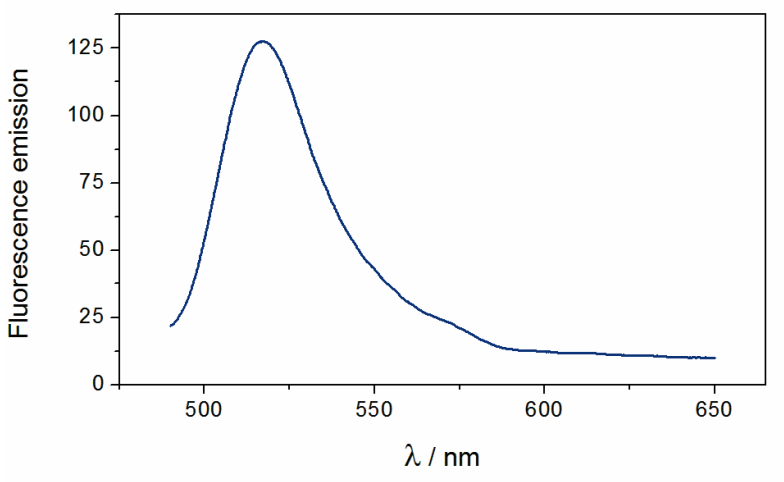

Figure S8. Bulk fluorescence emission spectrum for **DL hTR**.

Fluorescence lifetime measurements

Average fluorescence lifetime data for the donor fluorophore Alexa Fluor® 488 and acceptor Alexa Fluor® 594 in the full-length dual-labeled hTR construct **DL hTR** are presented in Table S3.

Table S3. Fluorophore average lifetimes in **DL hTR**.

Dual-labeled hTR construct	<τ> Alexa Fluor® 488 / ns	<τ> Alexa Fluor® 594 / ns
DL hTR	3.81 ± 0.02	4.18 ± 0.08

Average lifetimes are calculated according to Equation S4, where τ_i are the decay times obtained during the fitting process and p_i are the corresponding pre-exponential factors.

$$\langle \tau \rangle = \frac{\sum_i p_i \cdot \tau_i^2}{\sum_i p_i \cdot \tau_i} \qquad \text{(S4)}$$

The donor fluorophore Alexa Fluor® 488 is not heavily quenched. From the reported lifetime of the dye, 4.1 ns,[9] and the average lifetime quoted in Table S3, the average FRET efficiency for **DL hTR** can be estimated using Equation S5, where τ is the lifetime of the sample, and τ_0 is the donor lifetime in the absence of an acceptor.

$$E = 1 - \tau / \tau_0 \qquad \text{(S5)}$$

This gives an average FRET efficiency of 8%, taking into account the average lifetime of the donor, for **DL hTR**. This is an average value dictated largely by molecules in which a pseudoknot is not formed, and therefore where donor and acceptor are far apart, and will also be affected by any single-labeled molecules present containing only a donor

fluorophore. The average lifetime of the acceptor does not indicate a quenching of the dye, which could in principle be the cause of the apparent low FRET efficiency. The differences in FRET efficiency observed herein must therefore correspond to actual differences in distance between donor and acceptor fluorophore. However, a closer look at the global analyses revealed that bi-exponential functions were needed accurately to fit the decay traces, Table S4. A shorter decay time of about 1.3 ns was obtained in the Alexa Fluor 488® emission wavelengths, with a contribution of 6%. The acceptor Alexa Fluor 594® also showed a short decay time with a contribution of ~9%. This small fraction of partially quenched species may arise from interactions with surrounding nucleotides, which alter the local environment of the dyes.

Table S4. Fluorescence decay traces global analysis of **DL hTR**.*

Dual-labeled hTR construct	Emission wavelength / nm	τ_1 / ns (normalized pre-exponential)	τ_2 / ns (normalized pre-exponential)
DL hTR	515	3.95 (0.94)	1.30 (0.06)
	615	4.48 (0.91)	2.50 (0.09)

*Representative values at a single emission wavelength are presented, although the decay times were obtained from the global fit of 5 (for donor) or 3 (for acceptor) decay traces.

References

1. Li, H.; Ying, L.; Green, J.; Balasubramanian, S.; Klenerman, D. (2003) Ultrasensitive coincidence fluorescence detection of single DNA molecules. *Anal. Chem.*, **75**, 1664-1670.

2. Orte, A.; Clarke, R.; Balasubramanian, S.; Klenerman, D. (2006) Determination of the fraction and stoichiometry of femtomolar levels of biomolecular complexes in an excess of monomer using single-molecule, two-color coincidence detection. *Anal. Chem.*, **78**, 7707-7715.

3. Clarke, R.; Orte, A.; Klenerman, D. (2007) Optimized threshold selection for single-molecule two-color fluorescence coincidence spectroscopy. *Anal. Chem.*, **79**, 2771-2777.

4. Orte, A.; Clarke, R.; Klenerman, D. (2008) Fluorescence coincidence spectroscopy for single-molecule fluorescence resonance energy-transfer measurements. *Anal. Chem.*, **80**, 8389-8397.

5. Chen, J.; Greider, C. (2003) Template boundary definition in mammalian telomerase. *Genes Dev.*, **17**, 2747-2752.

6. Mitchell, J.; Wood, E.; Collins, K. (1999) A telomerase component is defective in the human disease dyskeratosis congenita. *Nature*, **402**, 551-555.

7. Kim, N.-K.; Zhang, Q.; Zhou, J.; Theimer, C. A.; Peterson, R. D.; Feigon, J. (2008) Solution Structure and Dynamics of the Wild-type Pseudoknot of Human Telomerase RNA. *J. Mol. Biol.*, **384**, 1249-1261.

8. Gavory, G.; Symmons, M. F.; Ghosh, Y. K.; Klenerman, D.; Balasubramanian, S. (2006) Structural Analysis of the Catalytic Core of Human Telomerase RNA by FRET and Molecular Modeling. *Biochemistry*, **45**, 13304-13311.

9. Molecular Probes The Handbook
   http://www.invitrogen.com/site/us/en/home/References/Molecular-Probes-The-Handbook.html